Session VIII

Wednesday, September 7 - morning

I8

BIOMINERALS IN THE LIGHT OF BRAGG COHERENT X-RAY DIFFRACTION IMAGING

V. Chamard

Aix-Marseille Université, CNRS, Centrale Marseille, Institut Fresnel, Marseille, France
virginie.chamard@fresnel.fr

Biomineralization integrates complex physico-chemical processes leading to an extraordinary diversity of calcareous biomineral crystalline architectures, in intriguing contrast with the consistent presence of a submicrometric granular structure [1]. Understanding how the mineral granules organize is a key element to gain knowledge on the biomineralization processes. While evidences for the existence of a mesoscale crystalline organization, spanning over a few granules, have been reported, a 3D image of the spatial organization of the crystalline domains is still lacking.

In this context, we have proposed to apply 3D X-ray Bragg ptychography microscopy [2], a recently demonstrated coherent diffraction imaging approach, based on the inversion of a set of intensity-only data [3]. Ptychography exploits the partially redundant information obtained by scanning a finite beam spot size transversally to the sample, while measuring the corresponding 3D far-field coherent diffraction pattern. Thereby, 3D imaging of extended crystalline samples becomes possible [4, 5].

In this presentation, we first briefly review the evolution of the Bragg ptychography approach, before detailing the results obtained in the framework of biomineralization. Specifically, we show the 3D images of the prismatic part of a *Pinctada margaritifera* shell, revealing this way the spatial arrangement of the crystalline structure with a nanometric resolution. We evidence a crystalline coherence extending over a few granules and further prove the existence of larger iso-oriented crystalline domains, slightly misoriented with respect to each other around a single rotation axis [6]. These original results bring new structural information, which will be discussed in the framework of recently proposed biomineralization growth schemes.

1.   Y. Dauphin, *Mineralogical Magazine* **72**, (2008), 243.

2.   P. Godard, G. Carbone, M. Allain, F. Mastropietro, G. Chen, L. Capello, A. Diaz, T. H. Metzger, J. Stangl and V. Chamard, *Nature Communications,* **2**, (2011), 568.

3.   P. Godard, M. Allain, V. Chamard, and J. Rodenburg, *Optics Express*, **20**, (2012), 25914.

4.   V. Chamard, M. Allain, P. Godard, A. Talneau, G. Patriarche and M. Burghammer, *Scientific Reports*, **5**, (2015), 9827.

5.   I. Pateras, M. Allain, P. Godard, L. Largeau, G. Patriarche, A. Talneau, K. Pantzas, M. Burghammer, A. A. Minkevich and V. Chamard, *Physical Review B*, **92**, (2015), 205305.

6.   F. Mastropietro, P. Godard, M. Burghammer, C. Chevallard, J. Daillant, J. Duboisset, M. Allain, P. Guenoun, J. Nouet, V. Chamard, *submitted*.

C24

NEW LABORATORY IMPLEMENTATIONS OF EDGE ILLUMINATION X-RAY PHASE CONTRAST IMAGING

G. K. Kallon,[1*] P. C. Diemoz,[1] M. Endrizzi,[1] F. A. Vittoria,[1] M. Wesolowski,[2] T. P. Millard,[1] D. Basta,[1] and A. Olivo,[1]

[1]*Department of Medical Physics and Biomedical Engineering, Malet Place, London WC1E 6BT*
[2]*Department of Medical Imaging, University of Saskatchewan, Saskatoon, SK, Canada, S7N 0W8*
*gibril.kallon.10@ucl.ac.uk

Edge illumination X-ray phase contrast imaging (EI XPCI) is a technique that enables quantitative retrieval of the absorption, differential phase and ultra-small angle X-ray scattering properties of an object using commercially available, polychromatic sources in a laboratory environment [1,2]. Two periodic masks, consisting of long, vertical slits are normally used. The first (sample) mask is placed before the sample and reshapes the incoming beam, while the second is placed just before the detector pixels, partially intercepting the beamlets, thereby making the system sensitive to refraction caused by the sample. A single image taken at a given sample mask displacement contains a mixture of absorption, differential phase and scattering effects. To retrieve the two (phase & absorption) or three (phase, absorption & scattering) channels of information, two or three images need to be acquired at different sample mask displacements and then mathematically combined.

In this presentation, we report on a new laboratory implementation of EI based on the use of a single mask. Besides simplifying the set-up and relaxing the system alignment constraints, it also enables phase and absorption retrieval through the simultaneous acquisition of two images in a single shot. This is realised by removing the second mask and using the boundary between detector pixels as the edge sensing mechanism (Fig. 1(a)). Figure 1(b) shows the image captured by a single mask EI system for all the detector pixels, and how alternating sets of pixels are then used to obtain a pair of images with inverted refraction contrasts. The single mask EI set-up can also potentially reduce the dose delivered to the sample by the current, "standard" double mask set-up by up to a factor of two, as only a single exposure is needed.

We will additionally show how two-directional EI sensitivity can be achieved by replacing the vertical slits with L-shapes and acquiring images at six different sample mask displacements [3]. This yields the refraction and scattering channels in both directions. In general, 2D differential phase images have the advantage of enabling easy phase integration and removing the streak artefacts common to the 1D case [4].

Furthermore, these developments can be combined with new detector technology, e.g. PixiRad a photon counter with a sharp PSF [5], and high-quality masks to improve the aforementioned set-ups. This will lead to the realisation of new designs (single mask 2D EI, dual-energy EI etc.) which even better exploit the advantages provided by the EI technique.
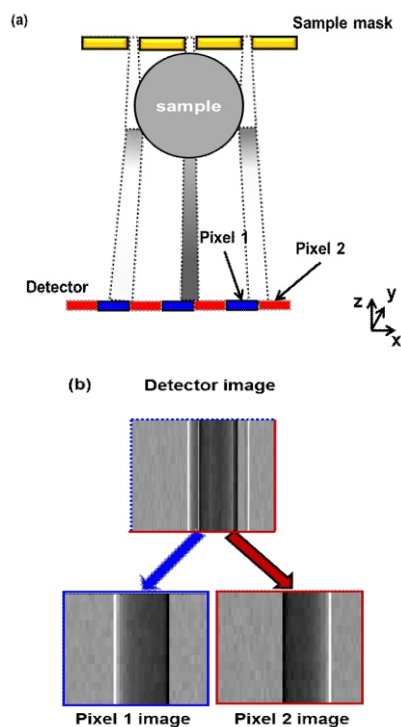

Figure 1. (a) Schematic for the single mask edge illumination set-up, (b) an unprocessed image using all detector pixels (top), and the images formed by the two sets of pixels (bottom).

1. A. Olivo & R. Speller, *Appl. Phys. Lett.*, **91**(7), (2007).

2. A. Olivo, K. Ignatyev, P.R.T. Munro, R. D. Speller, *Appl. Opt.*, **50,** (2011), pp. 1765-1769.

3. G. K. Kallon, M. Wesolowski, F. A. Vittoria, M. Endrizzi, D. Basta, T. P. Millard, P. C. Diemoz, A. Olivo, *Appl. Phys. Lett.*, **107**(20), (2015).

4. C Kottler, C David, F Pfeiffer, O Bunk, *Opt. Express*, **15**(3), (2007), pp. 1175-1181.

5. R. Bellazzini, G. Spandre, A. Brez, M. Minuti, M. Pinchera, P. Mozzo, *J. Instrum.*, **8**(02), (2013), C02028.

C25

SYRIS: A FLEXIBLE AND EFFICIENT FRAMEWORK FOR SIMULATING X-RAY IMAGING EXPERIMENTS

T. Faragó[1,2], P. Mikulík[3], A. Ershov[1,2], M. Vogelgesang[4], D. Hänschke[1,2], T. Baumbach[1,2]

[1]*Institute for Photon Science and Synchrotron Radiation, Karlsruhe Institute of Technology, Herrmann-von-Helmholtz-Platz 1, 763444 Eggenstein-Leopoldshafen, Germany*
[2]*Laboratory for Applications of Synchrotron Radiation, Karlsruhe Institute of Technology, Herrmann-von-Helmholtz-Platz 1, 763444 Eggenstein-Leopoldshafen, Germany*
[3]*CEITEC – Central European Institute of Technology, Masaryk University, Kotlářská 2, 611 37 Brno, Czech Republic*
[4]*Institute for Data Processing and Electronics, Karlsruhe Institute of Technology, Herrmann-von-Helmholtz-Platz 1, 763444 Eggenstein-Leopoldshafen, Germany*
tomas.farago@kit.edu

With *syris* we present a software tool to simulate the complete image formation process from an X-ray source through an arbitrary number of objects to a detector system. Our current implementation takes sample and beam motion, wavefield propagation, its detection process and coherence effects into account. This allows us to simulate a broad range of X-ray imaging experiments and their peculiarities like motion blur, beam drift and realistic noise.

Syris is organized as a framework and consists of basic abstract building blocks with a well-defined application programming interface (API) in Python. We provide implementations of all building blocks to conduct full virtual experiments. These implementations are optimized to achieve a reasonable compromise between efficiency and physical correctness. Moreover, they are written in OpenCL [1] and can thus be executed on numerous platforms, e.g. modern highly parallel GPUs which greatly speed up the computations. Users can provide their own implementations of this API which increases the framework's flexibility.

Combining flexibility with an efficient implementation makes *syris* a powerful tool to investigate novel imaging approaches [2, 3] and validate sophisticated data processing pipelines [4, 5]. Because the data processing parameters depend on experimental conditions, systematic studies of mutual dependencies will help to develop more robust algorithms optimized for particular scientific use cases.

To demonstrate the potential of the framework we first show the simulation of a high-speed radiography experiment conducted with different exposure times giving rise to varying noise levels. We then show the accuracy of a selected motion estimation algorithm as a function of the noise level. Afterwards we pick a noise level and optimize one of the algorithm's parameters to obtain the most accurate flow field. Finally, we employ *syris* to create a complex 3D resolution pattern and use it as a sample in a virtual tomographic experiment to investigate the impact of various imaging conditions on the precision of different reconstruction algorithms.

1. Stone, J. E., Gohara, D. & Shi, G. (2010). *Computing in science & engineering*, 12(1-3), 66–73.

2. Moosmann, J., Ershov, A., Altapova, V., Baumbach, T., Prasad, M. S., LaBonne, C., ... & Hofmann, R. (2013). *Nature*, 497(7449), 374-377.
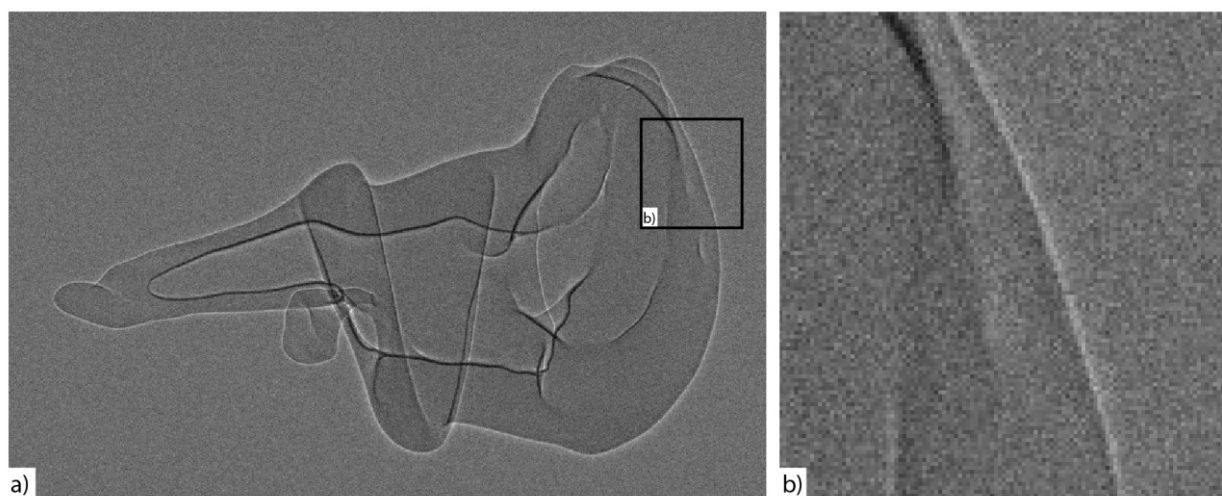
Figure 1. Simulation of a white beam X-ray radiograph of a biological screw joint found in Trigonopterus oblongus [6] based on data from a real CT measurement. The detailed crop in b) shows the appearance of realistic noise and the edge enhancement by free-space propagation visible as a white outlier on the sample boundary.

3. dos Santos Rolo, T., Ershov, A., van de Kamp, T. & Baumbach, T. (2014). *Proceedings of the National Academy of Sciences*, 111(11), 3921–3926.

4. Paganin, D., Mayo, S., Gureyev, T. E., Miller, P. R. & Wilkins, S. W. (2002). *Journal of microscopy*, 206(1), 33-40.

5. Van Nieuwenhove, V., De Beenhouwer, J., De Carlo, F., Mancini, L., Marone, F. & Sijbers, J. (2015). *Optics express*, 23(21), 27975– 27989.

6. van de Kamp, T., Vagovič, P., Baumbach, T. & Riedel, A. (2011). *Science*, 333(6038), 52-52.

C26

IN-SITU X-RAY TOMOGRAPHY STUDY OF CO_2 - INDUCED HEALING IN FRACTURED CEMENT

E. A. Chavez Panduro[1], M. Torsæter[2], K. Gawel[2], R. Bjørge[3], A. Gibaud[4], Y. Yang[5], Y. Zheng[6], H. O. Sørensen[5], D. W. Breiby[1]

[1]Norwegian University of Science and Technology, Høgskoleringen 5, 7491 Trondheim, Norway
[2]SINTEF Petroleum Research, Trondheim, Norway
[3]SINTEF Materials and Chemistry, Trondheim, Norway
[4]LUMAN, IMMM, UMR 6283 CNRS, Université du Maine, Le Mans Cedex 09, France
[5]University of Copenhagen, Department of Chemistry, Copenhagen, Denmark
[6]Technical University of Denmark, Department of Physics, Lyngby, Denmark
elvia.a.c.panduro@ntnu.no

The special report on Carbon Capture and Storage (CCS) published by the Intergovernmental Panel of Climate Change (IPCC) outlines that wells are among the most probable leakage paths from CO_2 storage reservoirs [1]. Whether they are in operation, or permanently plugged and abandoned, these wells are man-made structures of steel and cement that connect the storage reservoir with the atmosphere. If the steel or cement barriers break, leakage paths are likely to develop. To estimate potential leakage rates over time, and to optimize well remediation protocols, the compatibility of cement with CO_2 has been studied [2-5]. An important recent finding is that defects in cement (e.g. cracks) gradually heal when exposed to CO_2 [3-5]. The healing process, and its kinetics, has not yet been fully understood. In order to make use of this beneficial cement healing process in practice, a more detailed understanding is required of how and when it occurs. For that purpose we report in-situ μ-CT measurement in an environment of CO_2 saturated in brine to study both the carbonation and the healing processes on fractured cement.

Cement blocks with artificial channels were used to mimic fractures in cement. The sample was submerged in a saline solution (1%wt NaCl) inside the pressure cell and exposed to CO_2 for 20 hours at 50 bars and ambient temperature. Figure 1 shows that CO_2 exposure of cement induces $CaCO_3$ precipitation in all confined areas (e.g. in fractures, microcavities, non-connected pores and at cement/aluminum interfaces). The volume rate at which $CaCO_3$ precipitated was found to be 4.6×10^{-5} mm^3/min. High resolution μ-CT shows us a varying $CaCO_3$ content within carbonated front of cement block suggesting dissolution of $CaCO_3$ during CO_2 exposure.

1.   IPCC Special report on CO_2 Capture and Storage. Eds: B. Metz et al. Cambridge UniversityPress, (2005) 244 pp.

2.   B. G. Kutchko et al *Environmental Science & Technology* **42** (2008) 6237–6242.

3.   H. E. Mason et al .*Environmental Science & Technology* **47** (2013) 1745-1752.

4.   S.D.C. Walsh et al. *Int. J. Greenh. Gas Con.* **22** (2014) 176-188.

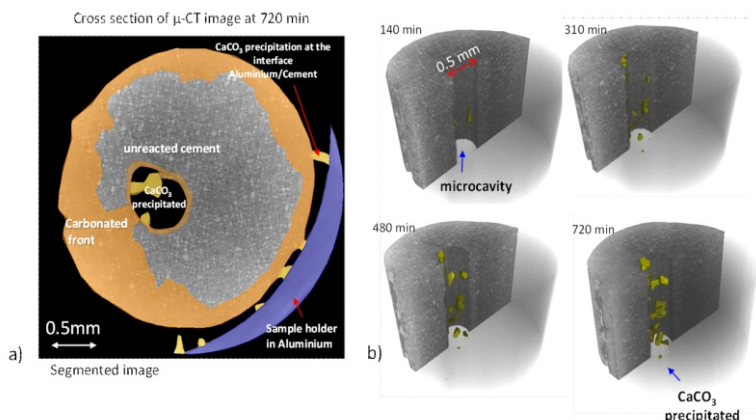5.   C. Kjøller et al. *Energy Procedia* **86** (2016) 342-351.

Figure 1. Results obtained from μ-CT. a) Cross section measured after 820 min, b) 3D representations of $CaCO_3$ precipitation in the microcavity as a function of time during the CO_2 exposure.